Overall viscoplastic behaviour of uranium dioxide

Jean-Marie Gatt, Jean-Claude Menard

CEA Cadarache DEN/DEC 13108 St Paul lez Durance, France

ABSTRACT:

This paper deals with the development of a uranium dioxide mechanical behaviour law. The purpose of this law, implemented into several design and research codes, is to improve the evaluation of in-core nuclear fuel thermal-mechanical performances. The overall expression of the law accounts for a grain size dependence, and is can operate under steady state and transient operating conditions. The porosity effect is introduced through a homogenization approach. Model parameter identification is performed from a creep compressive test on cylindrical samples, which are simulated using 3D finite element calculations. The mechanical behaviour is then validated on controlled strain rate tests. Test facility and modelling are in this paper. A good agreement was obtained between the simulation and experimental data.

INTRODUCTION

In order to understand the pellet cladding mechanical interaction during irradiation, finite element simulations of fuel elements are performed. To refine this approach, an improvement of fuel mechanical behaviour laws is necessary. The fuel is a porous ceramic, which becomes viscous above 900°C in compression and above 1300°C in traction (for a grain size of 8µm). From compression tests at high temperature (1000°C-1600°C) carried out on non-irradiated fuel pellets, we may observe different phenomena: during strain hardening tests, we observe either compressive peak or conventional curve stress versus strain (Fig. 8.) and during creep tests we observe (Fig. 1.):

- conventional creep response: a concave function strain versus time,
- conventional creep response due to great deformations of sample,
- a convex curves strain versus time.

The first models developed take only steady state conditions into account. In this framework, two steady state creep mechanisms have been identified: a scattering-creep mechanism (Nabarro[1]) and a dislocation-creep mechanism. This observation has led the authors[2][3] to propose the following steady creep behaviour law:

$$\dot{\varepsilon}_f = \frac{A_1}{d^2}\sigma e^{-\frac{Q_1}{RT}} + A_2\sigma^{4.5}e^{-\frac{Q_2}{RT}} \quad (1)$$

with A_i constant, Q_i activation energy for the scattering and dislocation mechanism. The first term concerns the scattering mechanism and second term, the dislocation mechanism. “d” is the average grain size of the material.
Sladkoff [4] proposes the following law:

$$\dot{\varepsilon}_f = \min(\max(\dot{\varepsilon}_{f1},\dot{\varepsilon}_{f2}),\dot{\varepsilon}_{f3}) \quad \text{with:} \dot{\varepsilon}_{fi} = A_i.d^{mi}.\sigma^{ni}.e^{k_i.f}e^{\frac{-Qi}{RT}} \quad (2)$$

f being the porosity volume fraction.
Using a more physical approach, linking microscopic observations and macroscopic mechanical behaviour, F. Dherbey [5] proposes:

$$\dot{\varepsilon}_f = \frac{\dot{\varepsilon}_0}{d^{1.3}}e^{-\frac{Q_1}{RT}}\mathrm{sh}\left(\frac{\sigma V}{kT}\right) \quad (3)$$

F. Sauter [6] has developed a complete model including transient and steady creep. He proposes a dislocation base-model which takes all the phenomena described above into account. Furthermore, he proposes a polycrystalline approach, based on modelling at the grain scale. He uses a self-consistence process to obtain overall mechanical behaviour.
More recently, Y. Monerie [7] takes porosity into account for steady creep using for each strain mechanism an elliptical thermo dynamical potential built from the hard sphere theory and the self consistence approach. These two strain mechanisms are coupled by a θ function depending on temperature and strain according to the Frost and Ashby [8] diagram. For each strain mechanism he obtains:

$$\begin{cases} \Psi_1 = \dfrac{K_1}{2d^2} e^{-\frac{Q}{RT}} \left(A_1(f) \left(\dfrac{3}{2} \sigma_m \right)^2 + B_1(f) \sigma_{eq}^2 \right) \\ \Psi_2 = \dfrac{K_2 d^2}{9} e^{-\frac{Q}{RT}} \left(A_2(f) \left(\dfrac{3}{2} \sigma_m \right)^2 + B_2(f) \sigma_{eq}^2 \right)^{9/2} \end{cases} \quad (4)$$

with: $\sigma_m = \dfrac{1}{3} \mathrm{tr}\, \sigma = \sum_i \sigma_{ii}$ and, $A(f) = \left(n\left(f^{-1/n} - 1 \right) \right)^{-2n/(n+1)}$ and, $B(f) = \left(1 + \dfrac{2}{3} f \right) (1-f)^{-2n/(n+1)}$ (n=1 et n=8)

$$\begin{cases} \Psi = (1-\theta)\Psi_1 + \theta \Psi_2 \quad \text{with} \quad \theta = \dfrac{1}{2} \left(1 + \mathrm{Tanh} \left(\dfrac{\bar{T} - T}{h} \right) \right) \\ \dot{\varepsilon}_{vp} = \dfrac{\partial \Psi}{\partial \sigma} = (1-\theta) \dfrac{\partial \Psi_1}{\partial \sigma} + \theta \dfrac{\partial \Psi_2}{\partial \sigma} + (\Psi_2 - \Psi_1) \dfrac{\partial \theta}{\partial \sigma} \\ \dot{f} = (1-f) \mathrm{tr} \dot{\varepsilon}_{vp} \end{cases} \quad (5)$$

This approach has been identified on 186 creep tests (Fig. 2.). One of the difficulties in this approach is the non-convexity of thermo dynamical potential. However, this problem doesn't appear in the application domain of this model. This paper proposes a generalisation of this last approach to model all phenomena described in Fig. 1. and Fig. 8.

OVERALL MECHANICAL BEHAVIOUR

To take transient creep into account, we propose to introduce a specific thermo dynamical potential as:

$$\Psi_p = \frac{K_p d^c}{a+1} e^{-\frac{Q}{RT}} \frac{\sigma^a}{\varepsilon_{eq}^b} \quad (6)$$

To take compression pick and a convex curves strain versus time into account, we propose to use "dynamic" θ function according this differential equation:

$$\dot{\theta} = \left(\frac{\theta_0 - \theta}{\theta_0} \right)^m \frac{1}{(m-1)\tau} \quad \text{with} \quad \theta_0 = \frac{1}{2} \left(1 + \tanh \left(\frac{\bar{T} - T}{h} \right) \right) \quad (7)$$

τ being a characteristic time and $\bar{T} = \omega \left(\dfrac{9A_1 \sigma_m^2 + 4B_1 \sigma_{eq}^2}{A_1 + 4B_1} \right)^{-q/2}$

Using Eq. (4) to Eq. (7) we obtain:

$$\begin{cases} \Psi = \Psi_p + (1-\theta)\Psi_1 + \theta \Psi_2 \\ \dot{\varepsilon}_{vp} = \dfrac{\partial \Psi}{\partial \sigma} = \dfrac{\partial \Psi_p}{\partial \sigma} + (1-\theta) \dfrac{\partial \Psi_1}{\partial \sigma} + \theta \dfrac{\partial \Psi_2}{\partial \sigma} \\ \dot{\theta} = \left(\dfrac{\theta_0 - \theta}{\theta_O} \right)^m \dfrac{\theta_0}{\tau} \quad \dot{f} = (1-f) \mathrm{tr} \dot{\varepsilon}_{vp} \end{cases} \quad (8)$$

The steady creep is reached when the time tends to infinity, we have:

$$\left. \begin{array}{l} \theta \to \theta_0 \\ \psi_p \to 0 \end{array} \right\} \Rightarrow \dot{\varepsilon}_{vp} = (1-\theta_0) \frac{\partial \Psi_1}{\partial \sigma} + \theta_0 \frac{\partial \Psi_2}{\partial \sigma} \quad (9)$$

We may point out that equation (6) is slightly different from Eq. (5); nevertheless this formulation (Eq. (8)) resolves the problem of convexity encountered in Eq. (5).

EXPERIMENTAL FACILITY

All the creep and hardening tests were conducted by compression on a screw-type Instron device, equipped with a suitably adapted furnace (fig. 9). The test atmosphere is controlled throughout the duration of the experiment at high temperature, with the objective of keeping the O/M ratio of the samples constant. The furnace, provided with a tungsten resistive heating element, runs under a reducing Ar/H_2 (5%) gaseous mixture flow, varying from 1100°C to 1700°C. The material used for the load train components extending into the furnace is also tungsten. Alumina spacers allow thermal insulation for the loading and pellet support. The test sample is set up at room temperature, between the tungsten loading platens, and a load of 5 MPa is applied first. The machine automatically maintains this constant load during heating. When the test temperature is reached and stabilised, a stress (creep test) or a constant strain rate (hardening test) is then applied with an automatic press system. Specimen length variation is measured by a transducer (LVDT) incorporated within the lower press loading system: a set of two extensometers measures the distance between the loading platens with a precision of 1 µm.

In this way, any possible creep deformation of the push rod is prevented from contributing to the measured pellet length evolution. The conventional strain value ($\Delta l/l_0$) is recorded by a computer. The furnace temperature is controlled using two thermocouples (temperature measurement [K] precision: ± 1%), one for regulation and one for measurement.

IDENTIFICATION OF PARAMETERS AND COMPARISON WITH TESTS

To identify parameters of the model, we use parameters identified for the first approach (Eq. 5.) and we identify parameters of transient creep and dynamic θ function with creep tests. We use finite element meshing of samples (Fig. 3.) to simulate compressive creep tests. For "dynamic" θ function we find m=2 and τ of the following form (Fig. 4): $\tau = \gamma_1 d^{-\gamma_2}$. Fig. 5. to Fig. 7. show at different temperatures, different stresses and for different grain sizes (Fig.7) a comparison between the simulation and the test results. We can observe that the simulation results are very close to experimental measurements. Fig. 8. shows a validation of model on controlled strain rate tests on different grain size samples.

CONCLUSION

We have proposed a new formulation for the overall mechanical behaviour of uranium dioxide. This model accounts for porosity (and its evolution under mechanical loading) and average grain size. For porosity, we have used a homogenisation approach to propose an analytical formulation. We have obtained a good agreement between the model and experimental results. However the modelling of transient creep and coupling between the two strain mechanisms use a macroscopic approach instead a pure physical approach. We shall focus on these points in the future to propose a micro-mechanical approach: from the grain mechanical behaviour to macroscopic mechanical behaviour.

ACKNOWLEDGMENTS

The present study was supported by CEA, EDF and AREVA_NP within the Pellet-Cladding Interaction program. The authors are indebted to Y. Monerie for his original ideas on the coupling of two strain mechanisms to take compression pick into account. The experimental teams of the CEA (DEC/SPUA) have been acknowledged for the quality of their results that have allowed us to validate the theoretical approach of UO_2 mechanical behaviour.

REFERENCES

1 Nabaro, R.R.N," Steady state diffusional creep", The philosophical Magazine, Vol. 16, 1967, pp.231-237

2 Bohaboy, P.E., Asamoto, R.R, Conti A.E: GEAP 10054, 1969

3 Tachibana, T., Yamada, K., Komatsu, J., Koizumi, M.: PNCT-831-72-02(1972)1/22, C.A.78(1973)N°118149; PNCT-831-72-03(1972)1/124;C.A.79(1973)N°120988

4 Sladkoff, M., Huet F., Mocellin, A., "Uniaxial compressive tests on non irradiated UO_2 nuclear pellet", personal communication, 2000

5 Dherbey, F., Louchet, F. , A. Mocellin, A., Leclercq, S., "Elevated temperature creep of polycrystalline uranium dioxide: from microscopic mechanism to macroscopic behaviour" , Acta Materialia 50, 2002,pp 1495-1505.

6 Sauter, F., Leclercq, S., Modeling, A. "Modeling of the non-monotonous viscoplastic behavior of uranium dioxide", J. of Nuclear Materials, Vol. 322, 2003, pp.1-14.

7 Y. Monerie, Y., JM Gatt, J.M.," Overall viscoplastic behaviour on non-irradiated porous nuclear ceramic", Mechanics of Materials, Vol.38, 2006, pp. 608-619.

8 Frost, H.J., Ashby, M.F., Chap 13: "Oxides with fluorite structure UO2 and ThO2, in deformation-mechanisms maps", Pergamon Press, Oxford, 1982, p93

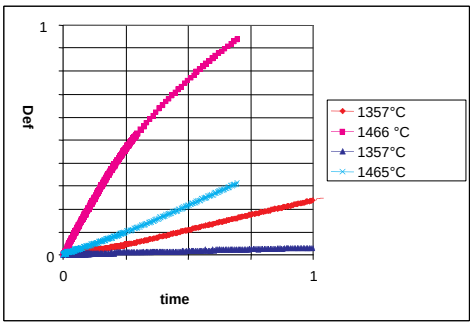

Figure 1: Behaviour at different grain sizes and different temperatures: great deformation, convex creep curve

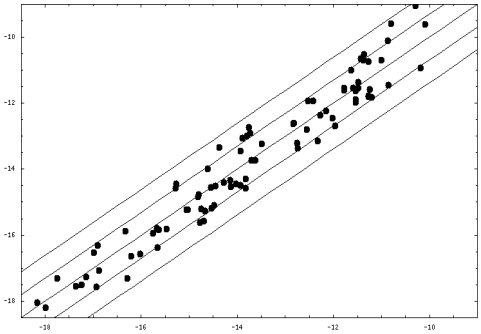

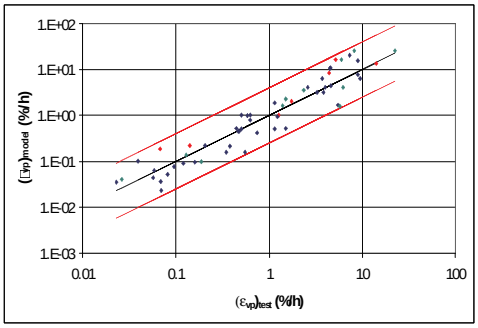

Figure 2: calculated strain rate versus test strain rate

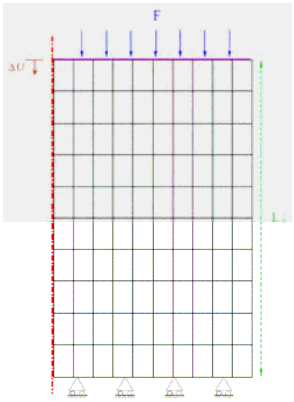

Figure 3: Meshing used to simulate creep tests

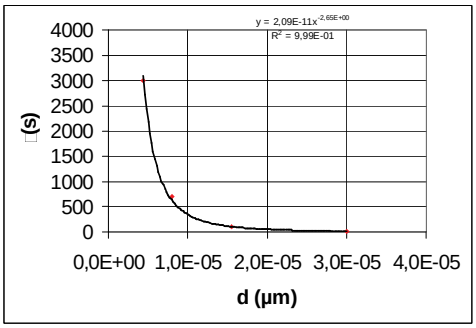

Figure 4: time characteristic versus grain size

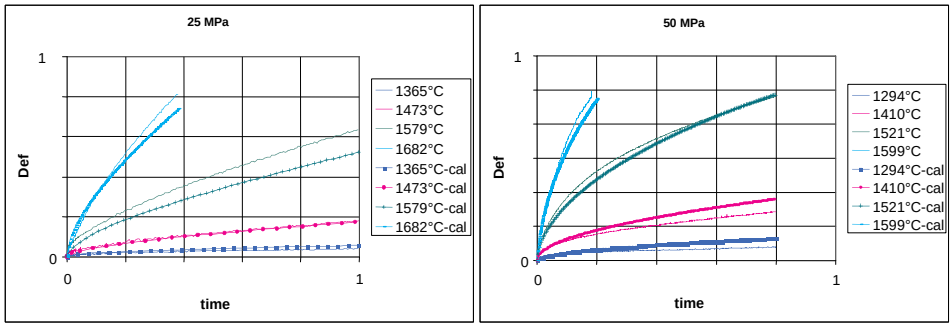

Figure 5: Simulation of creep tests 25 (8µm) and 50 MPa (30µm)

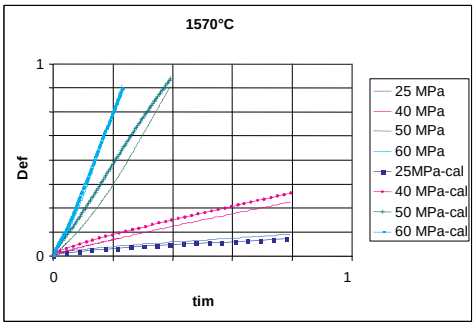

Figure 6: Simulation of creep tests at 1570 °C (8µm)

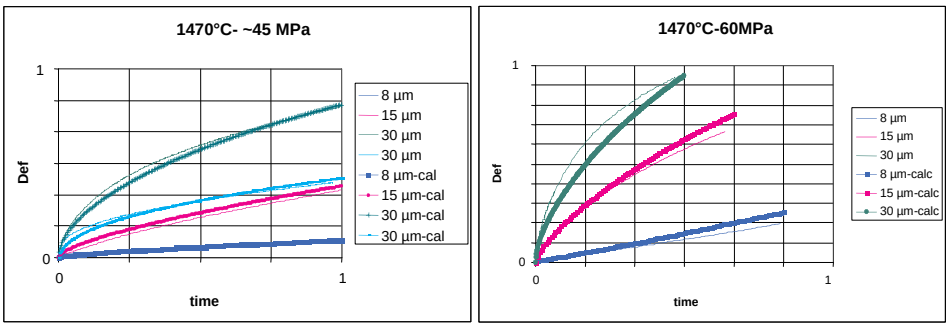

Figure 7: Simulation of creep tests at 1470 °C for different grain size samples

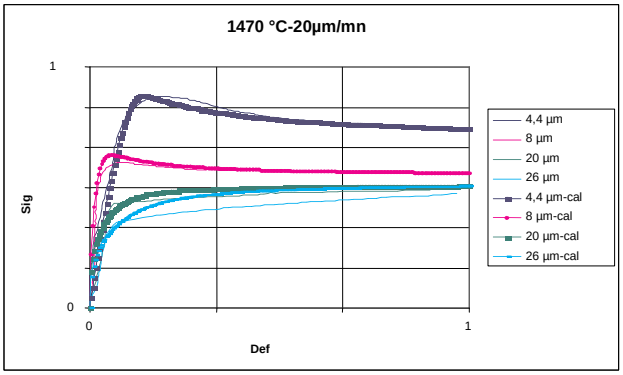

Figure 8: Simulation of controlled strain rate tests for different grain size samples

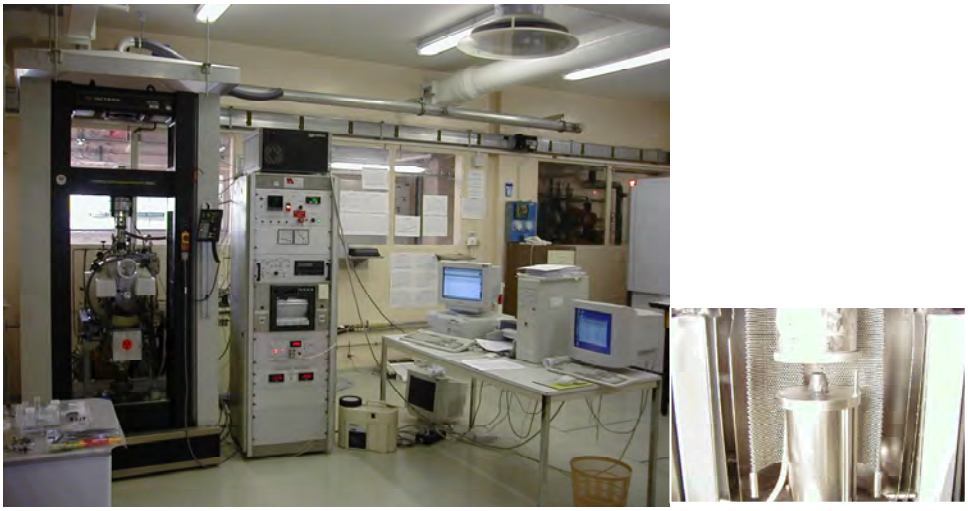

Figure 9: Pictures of high temperature creep equipment and loading push rods